# MEASUREMENT OF SMALL-ANGLE $p\bar{p}$ AND pp ELASTIC SCATTERING AT THE CERN INTERSECTING STORAGE RINGS

D. FAVART
Université Catholique de Louvain
B - 1348 Louvain-la-Neuve
Belgium

SUMMARY

The small angle elastic scattering of protons with protons and anti-protons has been measured at 52.8 and 30.4 GeV center-of-mass energy. Using the known total cross-section for pp scattering, a simultaneous fit to the $p\bar{p}$ and pp differential cross sections allows to determine the difference between the $p\bar{p}$ and pp total cross-sections and the ratio of the real-to-imaginary part of the pp and $p\bar{p}$ forward nuclear scattering amplitudes at both energies. In addition, the nuclear slope parameter at low momentum transfer is obtained for pp and $p\bar{p}$ at 52.8 GeV.

The comparison of proton-proton and proton-antiproton interactions at very high center-of-mass energies has been accessible to experiment over the last two years owing to the successful operation of the antiproton accumulator at CERN and the possibility to store a beam of antiprotons in one of the CERN intersecting storage rings (ISR). The Louvain-Northwestern collaboration [1] has endeavoured into a series of accurate measurements of $p\bar{p}$ and pp elastic scattering at small momentum transfer, aiming at the determination of the difference $\Delta\sigma$ between the $p\bar{p}$ and pp total cross-sections, the ratios $\rho(p\bar{p})$ and $\rho(pp)$ of the real to the imaginary part of the forward nuclear scattering amplitudes and the slopes $b(p\bar{p})$ and $b(pp)$ of the nuclear elastic differential cross-sections.

The experiment uses the method and part of the equipment of the CERN-Rome collaboration which, together with the Pisa-Stony-Brook collaboration, discovered the rise of the pp total cross-section at the ISR [2] and performed the measurement of the $\rho(pp)$ parameter [3]. Four miniature (48 x 28 $mm^2$) scintillator hodoscopes are installed above and below the two beams, in movable sections of the vacuum pipes ("Roman pots") at 8.7 m downstream of the intersection region. The pots and the hodoscopes can be accurately moved ($\pm$ 0.02 mm) under remote control and can approach the circulating beams to explore scattering angles down to 1 mrad. With the use of the Terwilliger focusing mode of momentum compaction, the spatial extension of the beam intersection region is much reduced. The triggering of the data acquisition can be simply made on the coincidence between the upper hodoscope in one arm and the lower one in the other and provides an almost background-free sample of elastic events. The luminosity of the intersection is monitored with four pairs of large (0.5 $m^2$) scintillator counters located symmetrically above and below the beam and carefully calibrated through the van der Meer beam vertical displacement method [4]. Such calibration was repeatedly performed during the pp and $p\bar{p}$ data taking runs, showing reproducibility at the percent level. Details on the apparatus, the information recorded, the background subtraction and the data reduction can be found elsewhere [5,6].

Data have been collected at three center-of-mass energies : $\sqrt{s}$ = 30.4, 52.8 and 62.3 GeV in successive pp and $p\bar{p}$ runs. During the $p\bar{p}$ runs, the antiproton beam intensity was of the order of 2 to 4 mA whereas the proton beam intensity was about 10 A, giving luminosities up to $7.10^{26}$ $cm^{-2}s^{-1}$.

For the pp runs, both beams were kept at 5 A resulting in a luminosity of about $5.10^{29}$ $cm^{-2}s^{-1}$. The total $p\bar{p}$ statistics collected was 1.7 $10^5$ elastic $p\bar{p}$ events at 52.8 and 62.3 GeV and 0.55 $10^5$ events at 30.4 GeV. The statistics of the pp comparison runs were of the order of $2.10^6$ events. We show in figs. 1 and 2, typical differential cross-sections observed for pp and $p\bar{p}$ collisions at $\sqrt{s}$ = 30.4 GeV and 52.8 GeV.

The data were fitted to the standard expression of the differential cross-section :

$$\frac{d\sigma}{dt} = \pi |f_C + f_N|^2 \qquad (1)$$

where the Coulomb amplitude $f_C$ and the nuclear elastic scattering amplitude $f_N$ at small momentum transfer squared t are parametrized in the usual way :

$$f_C = \mp 2\alpha \frac{G^2}{|t|} e^{\pm i\alpha\Phi} \qquad (2)$$

$$f_N = \frac{1}{4\pi} (i + \rho)\, \sigma_{tot}\, e^{bt/2} \qquad (3)$$

In the expression (2), $G = \left[1 + \frac{|t|}{0.71}\right]^2$ is the proton electromagnetic form factor and $\alpha\Phi$ is the Coulomb phase taken from reference 7 : $\alpha\Phi = \alpha\left[\ell n \frac{0.08}{|t|} - 0.577\right]$ ; the upper and lower signs are for pp and $p\bar{p}$ scattering respectively.

The results obtained at $\sqrt{s}$ = 52.8 GeV have already been published [6]. They were obtained through the simultaneous adjustment of expressions (1-3) to pp and $p\bar{p}$ data, using the known pp total cross section $\sigma_{tot}(pp)$ [8] as input to the fit and adjusting the following parameters : $\sigma_{tot}(p\bar{p})$, $\rho(pp)$, $\rho(p\bar{p})$, $b(pp)$, $b(p\bar{p})$, N, $\Delta h$. N is an overall normalization factor which allows for small event selection inefficiencies and absolute luminosity calibration error, and is assumed to be the same for pp and $p\bar{p}$ measurements ; and $\Delta h$ represents the mean deviation of hodoscope vertical separation from optical survey measurements and is essentially a correction to the t-scale. The procedure used in the analysis of the $\sqrt{s}$ = 30.4 GeV data is basically the same. However, at this energy the momentum transfer range explored is restricted to a maximum value $|t| \simeq 0.015$ $GeV^2$ and does not allow for an accurate determination of the nuclear slopes. The analysis of the $\sqrt{s}$ = 62.3 GeV run is still in progress.

The input to the fits and the results obtained are summarized in table 1. The errors shown are the statistical errors combined with the contribution of a possible 2 % systematic difference between pp and $p\bar{p}$ normalizations and a position uncertainty of the detectors of 0.02 mm between pp and $p\bar{p}$ runs. It should be noted that the total cross-section difference $\Delta\sigma$ is essentially independent of the $\sigma_{tot}(pp)$ input value, whereas $\sigma_{tot}(p\bar{p})$, given for convenience of comparison with similar data, directly depends on this input to the fit.

In fig. 3, we compare our results for $\Delta\sigma$ with lower energy data and a conventional fit [11] to these low energy data. The extrapolation of the latter which predict that $\Delta\sigma \to 0$ as $s \to \infty$, is in good agreement with our results. It has been observed [12], however, that one cannot yet exclude an unconventional contribution to the scattering amplitude (the so-called odderon [13]) which, at ISR energy, would be of the order of the odd-under-crossing Regge contribution to this amplitude and such that $|\Delta\sigma|$ would asymptotically become proportional to $\ell n s$. The $\Delta\sigma$ data at the highest energy accessible ($\sqrt{s}$ = 62.3 GeV) will be critical for this issue. We note also the agreement at $\sqrt{s}$ = 52.8 GeV between our value for $\Delta\sigma$ and the latest value reported by the CERN-Napoli-Pisa-Stony-Brook collaboration, $\Delta\sigma = 1.49 \pm 0.35$ mb [14]. In addition, the comparison of the total $p\bar{p}$ cross-section measured $\sqrt{s}$ = 30.4 and 52.6 GeV with the highest energy Fermilab data [10], shows conclusively that this cross-section is rising in the ISR energy domain. Indeed, the rate of increase of $\sigma_{tot}(p\bar{p})$ is compatible with a $\ell n^2 s$ behaviour, as fast as allowed by the Froissart bound.

The values of $\rho(pp)$ and $\rho(p\bar{p})$ measured in this experiment are displayed in fig. 4 together with previous data. It can be seen that $\rho(p\bar{p})$ is positive and increasing over the ISR energy range. This behaviour is predicted by models where both pp and $p\bar{p}$ total cross-sections are assumed to rise with rate close to the Froissart bound while $\Delta\sigma \to 0$ for $s \to \infty$. As an example, we show in fig. 4 the dispersion relation fit of Amaldi et al. [3] which is made under these assumptions.

It has been observed earlier [16] that the values of the low-t slopes, b(pp) and $b(p\bar{p})$, measured at $\sqrt{s}$ = 52.8 GeV are not significantly different from each other, as expected if the ratio of the widths of the diffraction peak approach unity at high energy ; this prediction of asymptotic theorems [17]

seems already fulfilled at ISR energies at the level of experimental accuracy. Finally, the elastic cross-section $\sigma_{el}$ can be determined from our measurement, through integration of the differential elastic cross-section. We find that the ratio of the elastic cross-section to the total cross-section is the same for pp and $p\bar{p}$, within experimental errors, and close to the values previously obtained at lower energy ($p_{lab} \gtrsim 100$ GeV/c), a feature predicted by optical models with goemetrical scaling.

REFERENCES

[1] D. Favart, C. Leroy, P. Lipnik, J.P. Matheys (Université Catholique de Louvain, B - 1348 Louvain-la-Neuve, Belgium), N. Amos, M. Block, D. Miller, S. Shukla, S. Zucchelli (Northwestern University, Evanston, Illinois 60201), G. Bobbinck, K. Potter, C. Vandervelde-Wilquet+(CERN, CH - 1211 Geneve 23, Switzerland), M. Botje, F. Linde (State University, Utrecht, The Netherlands).

[2] U. Amaldi et al., Phys. Lett. 44B, 112 (1973).
S.R. Amendolia et al., Phys. Lett. 44B, 119 (1973).

[3] U. Amaldi et al., Phys. Lett. 66B, 390 (1977).

[4] P. Bryant and K. Potter, CERN Internal Report ISR-ES-BOM/82-15.

[5] D. Favart et al., Phys. Rev. Lett. 47, 1191 (1981).

[6] N. Amos et al., Phys. Lett. 120B, 460 (1983).

[7] G.B. West and D.R. Yennie, Phys. Rev. 172, 1413 (1968).
The calculation of the Coulomb phase was recently examined by R. Cahn, CERN TH-3292 (1982),who uses an eikonal model and finds only small corrections to the West and Yennie result.

[8] U. Amaldi and K.R. Schubert, Nucl. Phys. B166, 301 (1980).

[9] W. Galbraith et al., Phys. Rev. 138B, 913 (1965).
S.P. Denisov et al., Nucl. Phys. B65, 1 (1973).

[10] A.S. Carroll et al., Phys. Lett. 80B, 423 (1979).

[11] W. Bartel and A.N. Diddens, CERN Internal Report NP/73-4.

[12] P. Gauron and B. Nicolescu, Orsay preprint IPNO/TH, 82-45.

[13] L. Lukaszuk and B. Nicolescu, Nuovo Cimento Letters 8, 405 (1973).

[14] M. Ambrosio et al., Phys. Lett. 115B, 495 (1982).

[15] K.J. Foley et al., Phys. Rev. Lett. 19, 857 (1967).
G.G. Beznogikh et al., Phys. Lett. 39B, 411 (1972).
V. Bartenev et al., Phys. Rev. Lett. 31, 1367 (1973).
U. Amaldi et al., Phys. Lett. 66B, 390 (1977).

+ present address : IIHE, Université Libre de Bruxelles, Belgium

J.P. Burq et al., Phys. Lett. 109B, 124 (1982).
L.A. Fajardo et al., Phys. Rev. D24, 46 (1981).

[16] A. Martin, Z. Phys. C15, 185 (1982).

[17] H. Cornille and A. Martin, Phys. Lett. 40B, 671 (1972).

Table 1

Input and result of the simultaneous fit to the pp and $p\bar{p}$ differential elastic cross-section data. Results at 30.4 GeV are preliminary.

| $\sqrt{s}$(GeV) | 52.8 | 30.4 |
|---|---|---|
| Input | $\sigma_{tot}(pp) = 42.67$ mb | $\sigma_{tot}(pp) = 40.14$ mb<br>$b(pp) = 12.2$ GeV$^{-2}$<br>$b(p\bar{p}) = 12.6$ GeV$^{-2}$ |
| Result | $\Delta\sigma = 0.98 \pm 0.36$ mb<br>$\sigma_{tot}(p\bar{p}) = 43.65\pm0.41$ mb<br>$\sigma_{el}(p\bar{p}) = 7.36\pm0.30$ mb<br>$\rho(pp) = 0.060\pm0.0006$<br>$\rho(p\bar{p}) = 0.101\pm0.018$<br>$b(pp) = 12.85\pm0.12$ GeV$^{-2}$<br>$b(p\bar{p}) = 13.36\pm0.53$ GeV$^{-2}$ | $\Delta\sigma = 1.5 \pm 0.5$ mb<br>$\sigma_{tot}(pp) = 41.7\pm0.5$ mb<br>$\sigma_{el}(p\bar{p}) = 7.1\pm0.3$ mb<br>$\rho(pp) = 0.040\pm0.005$<br>$\rho(p\bar{p}) = 0.031\pm0.021$ |

FIGURE CAPTIONS

Fig. 1. The measured differential cross-section $d\sigma/dt$ for elastic scattering of protons on protons (upper) and antiprotons (lower) at $\sqrt{s}$ = 52.8 GeV, as a function of $|t|$.

Fig. 2. Same as fig. 1 for $\sqrt{s}$ = 30.4 GeV.

Fig. 3. The difference $\Delta\sigma = \sigma_{tot}(p\bar{p}) - \sigma_{tot}(pp)$ versus laboratory momentum $P_{lab}$ [9, 10, 14]. The curve is the result of the fit of Bartel and Diddens [11] to the lower energy data.

Fig. 4. The parameter $\rho$ for pp and $p\bar{p}$ scattering [15] as a function of $\sqrt{s}$. For clarity, the pp data of Fajardo et al. which lie above the other pp data have been omitted. The curve is the result of the dispersion relation fit of Amaldi et al. [3] to total cross-section and $\rho$ data.

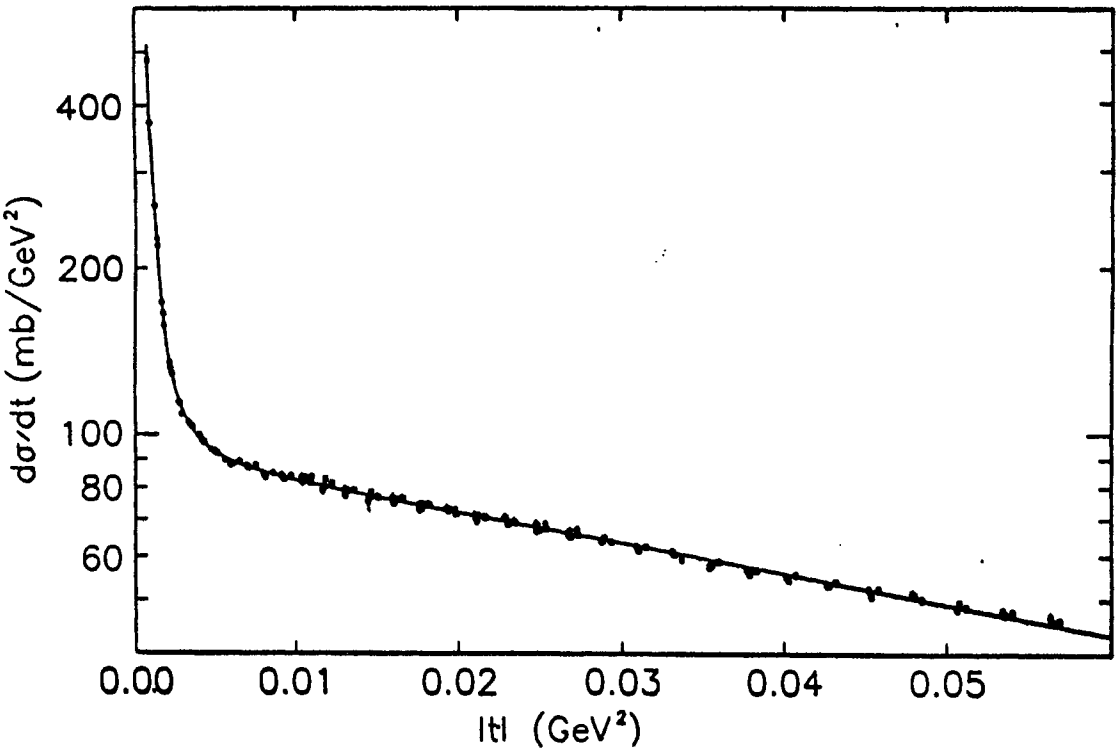
400
200
100
80
60
dσ/dt (mb/GeV²)
0.00
0.01
0.02
0.03
0.04
0.05
|t| (GeV²)

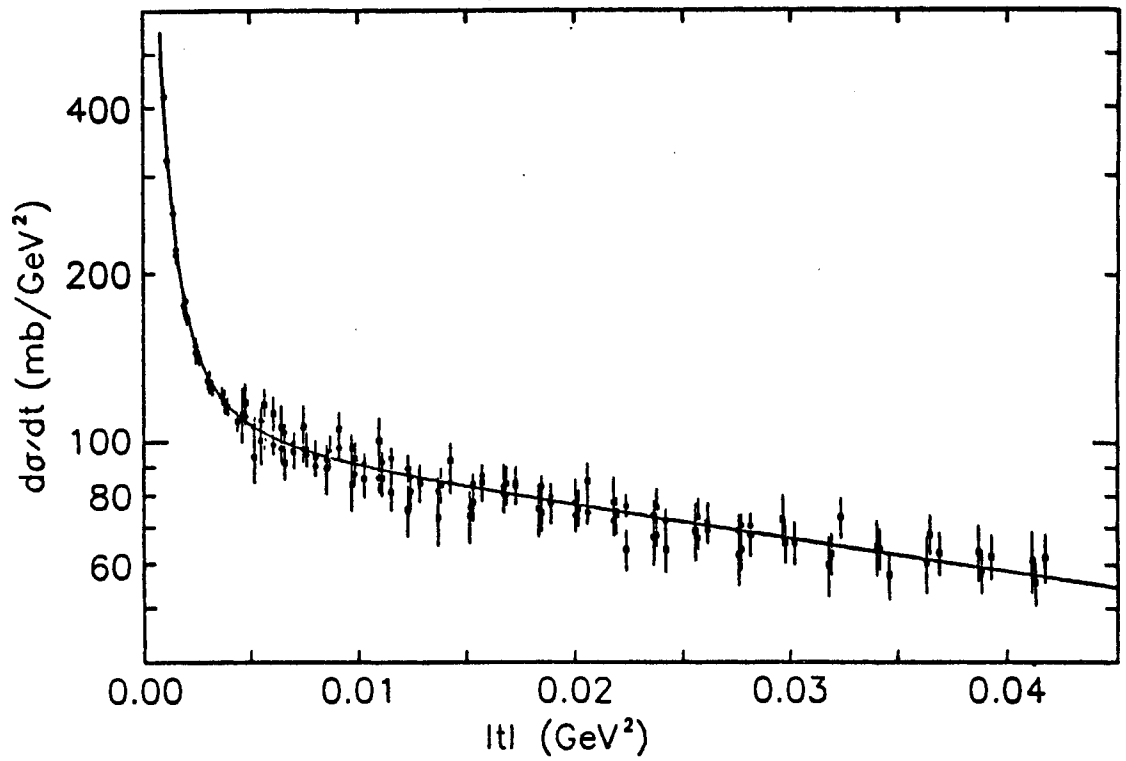
400
200
100
80
60
dσ/dt (mb/GeV²)
0.00
0.01
0.02
0.03
0.04
|t| (GeV²)

Fig. 1

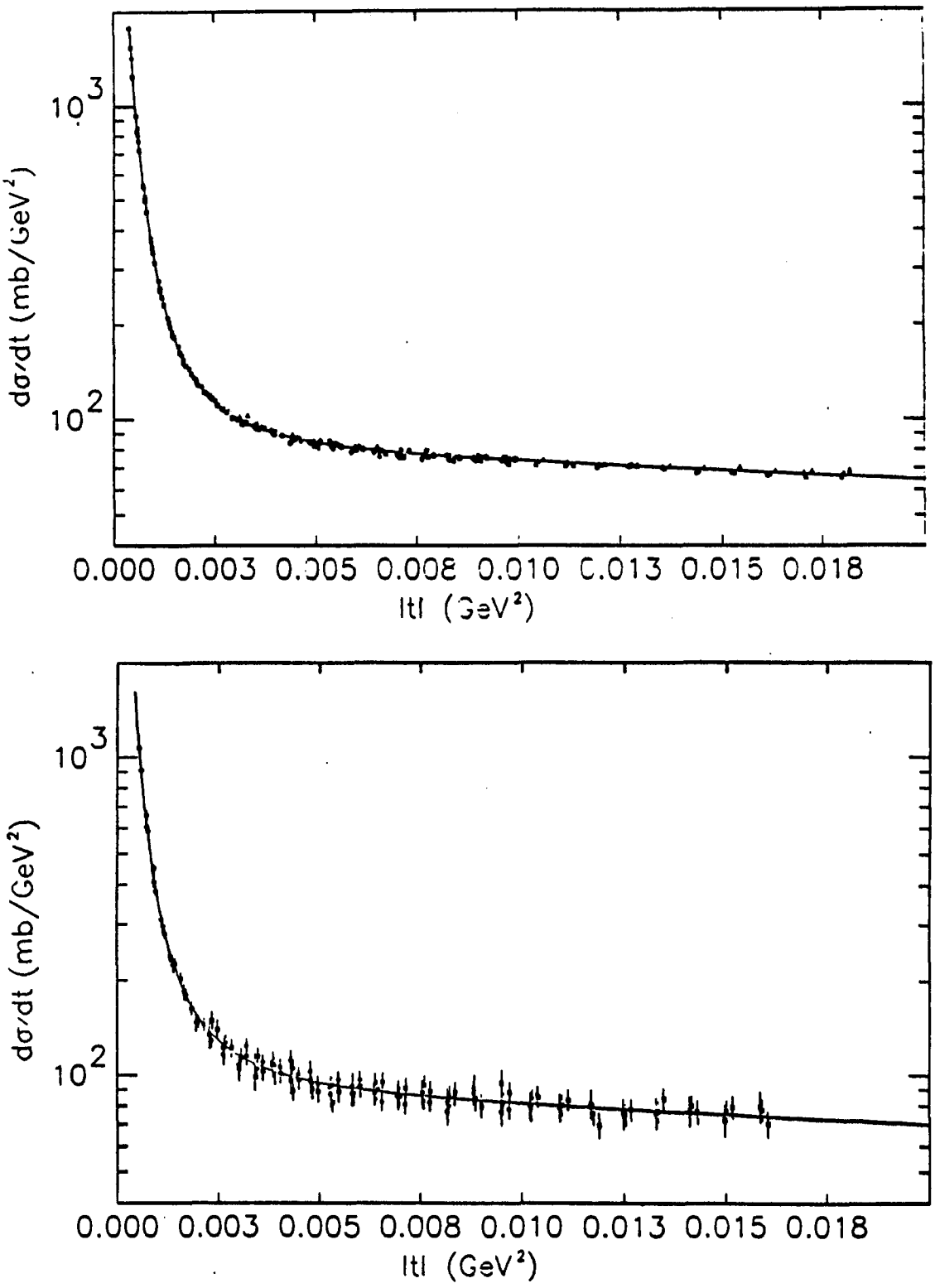
$10^3$
$10^2$
dσ/dt (mb/GeV²)
0.000 0.003 0.005 0.008 0.010 0.013 0.015 0.018
|t| (GeV²)
$10^3$
$10^2$
dσ/dt (mb/GeV²)
0.000 0.003 0.005 0.008 0.010 0.013 0.015 0.018
|t| (GeV²)

Fig. 2

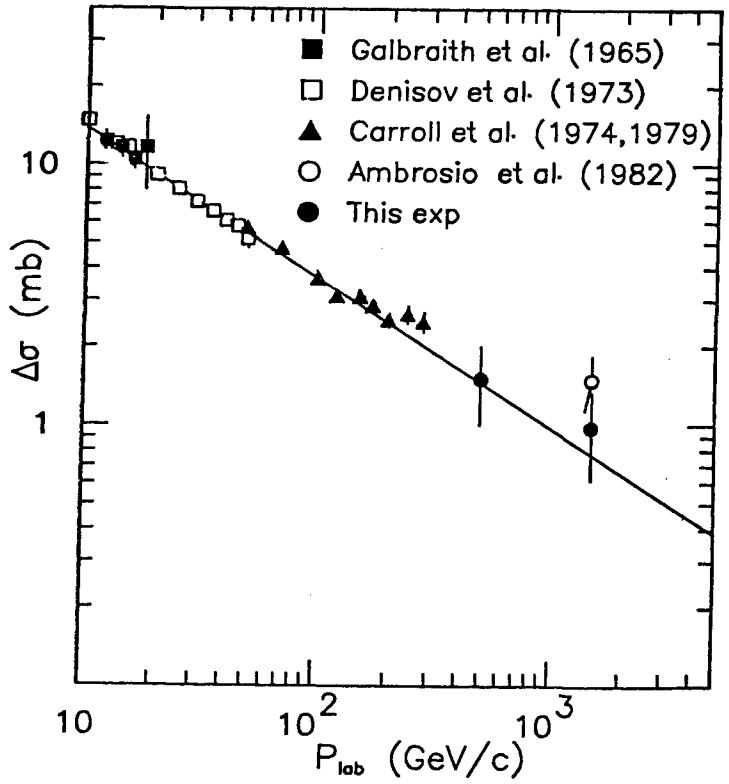
Galbraith et al. (1965)
Denisov et al. (1973)
Carroll et al. (1974,1979)
Ambrosio et al. (1982)
This exp
10
1
Δσ (mb)
10
10^2
10^3
P_lab (GeV/c)

Fig. 3

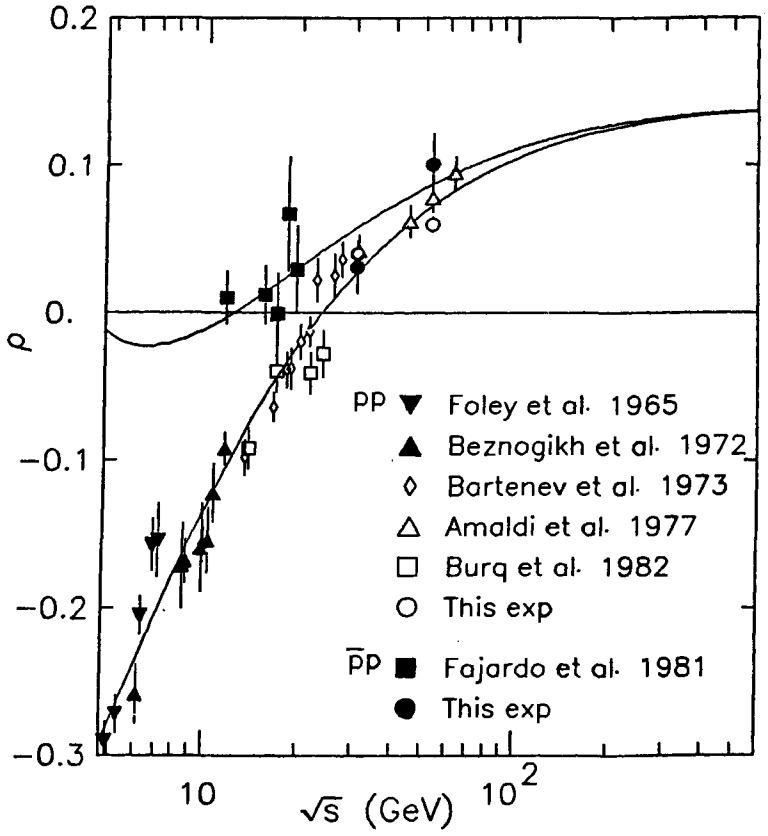
0.2
0.1
0.
−0.1
−0.2
−0.3
ρ
pp
Foley et al. 1965
Beznogikh et al. 1972
Bartenev et al. 1973
Amaldi et al. 1977
Burq et al. 1982
This exp
p̄p
Fajardo et al. 1981
This exp
10
10^2
√s (GeV)

Fig. 4